Deposition and Characterization of MoS_2 Thin Film on SiO_2/Si and Si Substrates via Spin Coating Method: A Comparative Study

*Vaibhav Y. Borokar[1], Bhushan B. Desale[1], Deepashri Torawane[2], Pankaj Waghmare[3], Viral Barhate[4], Vilas Patil[5], Ashok M. Mahajan[1]**

[1]Department of Electronics, Kavayitri Bahinabai Chaudhari North Maharashtra University, Jalgaon
[2]A.C. Patil College of Engineering, Kharghar, Navi Mumbai
[3]BP Arts, SMA Sciences and KKC College, Chalisgaon
[4]Department of Physics and Electronics, Arts, Science & P.O. Nahata Commerce College, Bhusawal
[5]Tyndall National Institute, Cork
**Corresponding Author: ammhajan.ele@gmail.com*

Abstract

In this study, we report the deposition and comparative characterization of molybdenum disulfide (MoS_2) thin films on SiO_2/Si and bare Si substrates using the spin-coating method. MoS_2 a two-dimensional transition metal dichalcogenide, exhibits promising electronic and optoelectronic properties, making it a strong candidate for next-generation semiconductor devices. A uniform precursor solution was spin-coated under controlled conditions, followed by post-deposition annealing to enhance crystallinity and film quality. The structural, morphological, and optical properties were systematically analyzed using X-ray diffraction (XRD), Raman spectroscopy, Fourier-transform infrared spectroscopy (FTIR), and atomic force microscopy (AFM). FTIR spectra revealed progressive enhancement of Mo–S vibrational modes with increasing coating duration, confirming improved nucleation and uniform deposition, particularly on SiO_2/Si substrates. Raman analysis identified the characteristic E_2g^1 and A_1g modes of 2H-MoS_2, though their weak intensity compared to strong Si substrate peaks indicated partial coverage, structural disorder, and nano crystallinity. XRD confirmed the crystalline 2H-MoS_2 phase, with reflections matching standard JCPDS data, and showed that longer deposition times enhanced crystallinity, c-axis orientation, and film quality without impurity phases. Overall, MoS_2 films on MoS_2/Si exhibited superior layer formation and uniformity compared to bare Si, underscoring the critical role of substrate choice in film growth and the optimization of device performance

Keywords: *SiO_2/Si and Si Substrate, Molybdenum disulfide (MoS_2), Spin coating, FTIR, XRD, Raman spectroscopy etc.*

1. Introduction:

Since the discovery of graphene, there has been an ever-increasing interest in two-dimensional (2D) layered materials with exceptional properties. To this end, a variety of synthesis methods have been developed [1-4]. However, it is still challenging to produce large-scale high-quality single-crystalline 2D materials. Electronic technology continuously demands the novel materials and novel architectures for further scaling of the advanced technology. Silicon based devices have been at the frontend of device technologies for last five decades, allowing for continuous scaling up to nano level. This scaling phenomena such as short channel effects, leakage currents and quantum phenomena in the nanometer regime pose significant barrier to further scaling and improvement of transport properties.[5] In recent years, a lot of research has been done on the graphene;2D material research was investigated followed by isolation of Graphene. This new 2D content includes transition metal dichalcogenides, 2D sheets and many carbide and nitride-based materials such as MoS_2, WS_2, $MoSe_2$, WSe_2 and BN [6]. The number of investigations related to this 2D material has increased tremendously over the last decades. The high quality 2D/oxide interfaces are critical to electronic devices such as radio-frequency transistor and flexible electronics [7]. 2D content generally shows poor electronic properties with less mobility, less stability and high contact resistance that requires further study and optimization before effectively competing in real-world technology. Molybdenum disulfide (MoS_2), a member of the transition metal dichalcogenides (TMDCs), offers several advantages due to its unique and tunable electronic properties. Structurally, MoS_2 can be described by a simple model in which each molybdenum (Mo) atom is covalently bonded to three sulfur (S) atoms above and three S atoms below in a prismatic configuration [8].

Thin film deposition is the process of making a thin layer of material that can be as thin as a fraction of a tiny nanometer or as thick as a few micrometers on a base material. Different ways of putting down thin films have an effect on how they look and feel. One way is called Atomic layer deposition (ALD). With ALD you can control the thickness of the film very precisely. This is because the process involves putting down thin layers one after the other using special vapors that react in a controlled way on the surface. ALD also has the advantage of making large sheets of different types of inorganic films such as oxides nitrides metals and chalcogenides. [9-15]. MoS2 thin films with a few monolayers have been obtained by mechanical exfoliation [16], physical vapor deposition [17], Chemical Vapor Deposition (CVD) [18], RF sputtering [19, 20], Spin Coating [21-23] etc. Spin coating is a common method for making thin even layers on flat surfaces. Recently nanomaterials have become more popular. They are being used in a simple and direct way to deposit different types of materials like semiconductors metal, nanoparticles, nanowires, carbon nanotubes, quantum dots, grapheme, and two- dimensional flakes [24]. In a regular spin coating process a small amount of liquid is placed in the middle of a surface. In a typical spin coating process a small amount of liquid is placed in the center of a surface. Next the surface is rotated quickly (usually between 1000 to 6000 revolutions per minute). The spinning force evenly spreads the solution across the whole surface. As the liquid dries up it leaves behind a thin layer of the materials you want. The film's thickness on a surface can vary based on the

solution type spinning speed and surface material. It can vary in size from very small units called nanometers to slightly larger units called micrometers [25]. Spin coating is a common way to make see-through electrodes thin-film transistors and quick lasers with 2D material mixtures. It is important to closely manage how thick the film is and how it looks on the surface for these uses [26, 27]. A single layer of MoS_2 forms when this prismatic structure repeats infinitely along a plane, creating a layer where a central plane of Mo atoms is sandwiched between two planes of S atoms. While the bonds between atoms within a single layer of MoS_2 are covalent, additional layers stack through van der Waals interactions, which are weaker than the covalent bonds within each layer. [28]. MoS_2 primarily exists in two phases: a trigonal prismatic structure (2H-MoS_2) and an octahedral structure (1T-MoS_2). These phases exhibit distinct electronic properties, with the 2H-MoS_2 phase being semiconducting, while the 1T-MoS_2 phase is metallic. [29]. In [30], Eda et al. demonstrated that 2H/1T hybrid structures can coexist within chemically exfoliated MoS_2 nanosheets. Scalable production of two-dimensional (2D) materials, such as MoS_2, can be achieved through solution-based exfoliation methods [31]. MoS_2 has a lot of potential for uses in solutions that haven't been fully explored yet. [32]. MoS2 can be used in photoluminescence, photovoltaic, and photocatalytic research since it is a multilayer semiconductor material with excellent light absorption [33]. The electronic structure, physical, and optical characteristics of MoS_2 would be greatly influenced by the number of layers and substrate environment, which would also have an impact on the optical device's performance [34]. Studies on the optical characteristics of MoS_2 are currently few. Therefore, in an effort to comprehend the luminescence laws of MoS_2, research has been conducted on its use on SiO_2/Si and sapphire substrates at various laser wavelengths and powers [35]. In the present work, we report Deposition of MoS_2 thin film on SiO_2/Si and Si Substrates by Spin Coating. The deposited thin films were subsequently characterized by using Fourier transform infrared spectroscopy (FTIR), Atomic Force Microscopy (AFM), Micro- Raman Spectra and X-ray diffraction (XRD).

2. Experiments details:

2.1 Method for SiO_2/Si and Si substrate cleaning:

Silicon dioxide (SiO_2) was deposited on silicon (Si) using low-pressure chemical vapor deposition (LPCVD) to achieve a thickness of 280 nm. Subsequently, molybdenum disulfide (MoS_2) films were grown on both SiO_2/Si and Si substrates using a spin-coating system. The standard substrate cleaning process (SCP) was followed to eliminate dust particles and contaminants, utilising acetone and deionized (DI) water for cleaning. We successively repeated this cleaning process four times.

2.2 Synthesis Method of MoS2:

All of the chemical reagents used in this experiment were analytical grade. In a typical synthesis, 1.50 g of Ammonium Molybdate and 1.00 g of Thiourea were dissolved in 30 mL deionized water, and then 10 mL ethanol, and 10 mL N–Methyl pyrrolidone (or 10 mL ethylene glycol) were added into the solution. Subsequently, the solution was stirred for a few minutes until it was mixed uniformity. Then they obtained solution was transferred into a 100 mL Teflon–lined

stainless steel autoclave and sealed tightly, heated at 250 ◦C for 8 h. After cooling naturally, the black precipitate was collected by filtrate, washed with deionized water and ethanol, and dried in an oven at 60 ◦C for 6 h. The dried samples were annealed in a conventional tube furnace at 400 ◦C for 1 hr.

2.3 Deposition Method of MoS2 by Spin Coating:

20 mg of MoS_2 powder was taken and 500 µL of IPA and 500 µL of DI water added for sonication. This mixture was **sonicated** for 10 minutes, and then 50 µL of the solution was taken with a pipette for spin coating.

The results are reported for SiO_2/Si and Si samples prepared at various spin speeds (rpm) and deposition times (seconds) in the following table T1. The details of the deposition parameters are as follows:

Table 1: Deposition Parameters for MoS_2 thin Films on Si and SiO_2/Si Substrates Using Spin Coating at 3000 rpm.

Sr. No.	Sample Description	Stage	Spin Speed (rpm)	Time (sec)	Sample ID
1	MoS_2 on Si	Stage 1	3000	40	Sample 1
2	MoS_2 on Si	Stage 2	3000	50	Sample 2
3	MoS_2 on Si	Stage 3	3000	60	Sample 3
4	MoS_2 on SiO_2/Si	Stage 4	3000	40	Sample 4
5	MoS_2 on SiO_2/Si	Stage 5	3000	50	Sample 5
6	MoS_2 on SiO_2/Si	Stage 6	3000	60	Sample 6

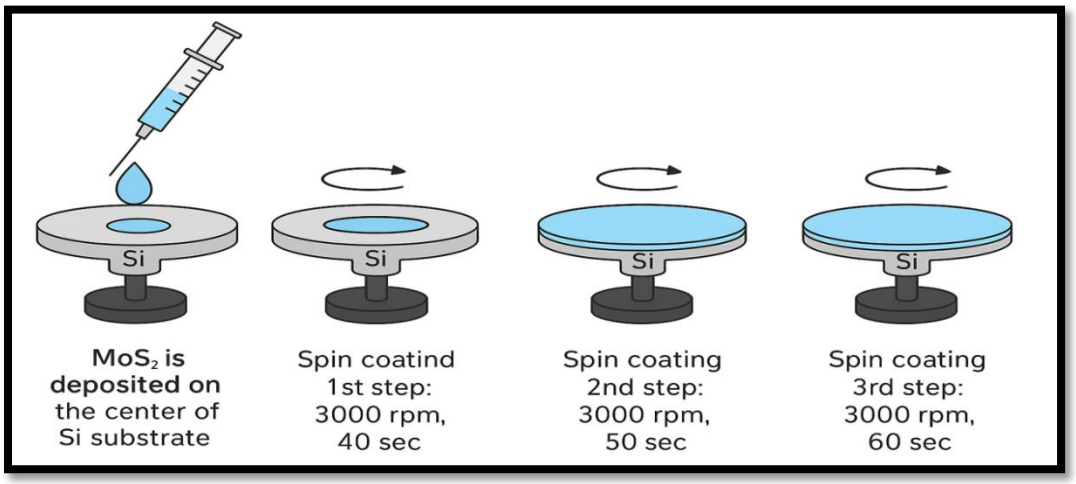

Fig.1 Shows Step-by-step schematic of the spin coating process used for the deposition of MoS_2 thin films on a Si substrate.

A droplet of MoS_2 solution is first dispensed at the center of the Si substrate. The substrate is then subjected to three sequential spin-coating steps at a constant speed of 3000 rpm for durations of 40 seconds, 50 seconds, and 60 seconds, respectively. The centrifugal force during each cycle spreads the solution uniformly, resulting in the formation of a homogeneous MoS_2 thin film layer.

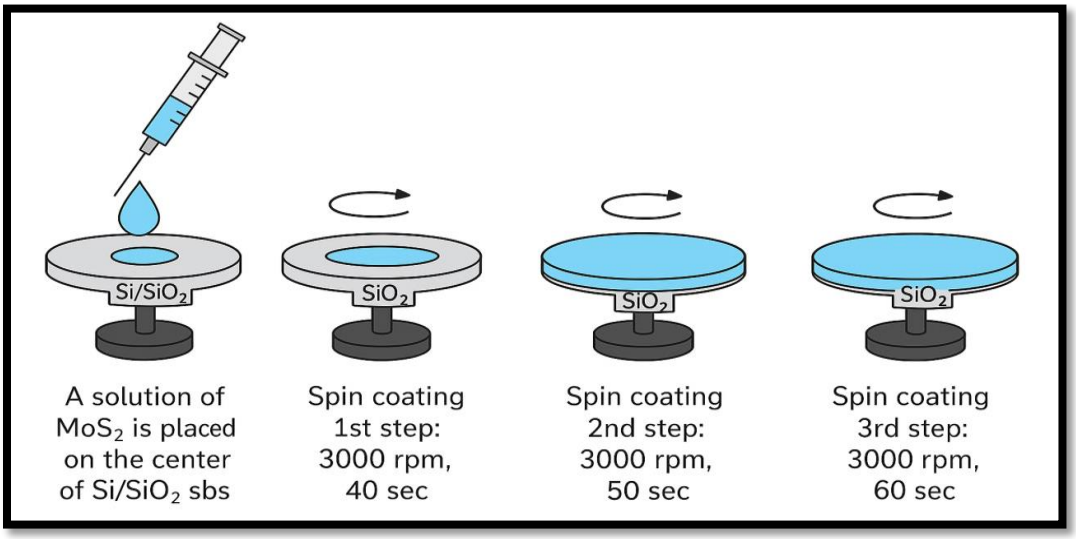

Fig.2 Shows stepwise illustration of MoS_2 thin film deposition on a SiO_2/Si substrate using the spin coating method.

Above schematic diagram represent the spin-coating process for depositing MoS_2 thin films on a SiO_2/Si substrate. The process involves dropping a MoS_2 solution on the substrate, followed by three spin coating steps at 3000 rpm for 40s, 50s, and 60s, respectively. This step-by-step process ensures uniform spreading and formation of the MoS_2 thin film.

3. Results and discussion:

3.1 Fourier Transform infrared Spectroscopy (FTIR)

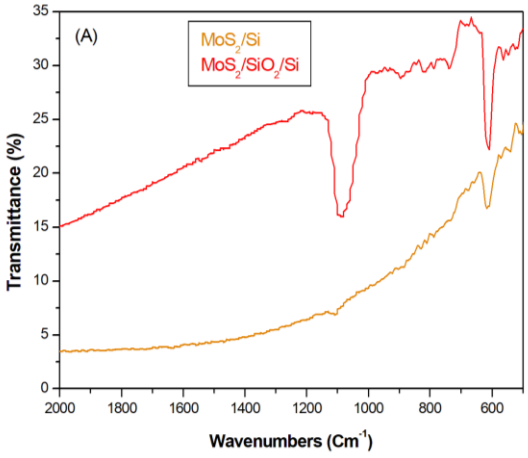

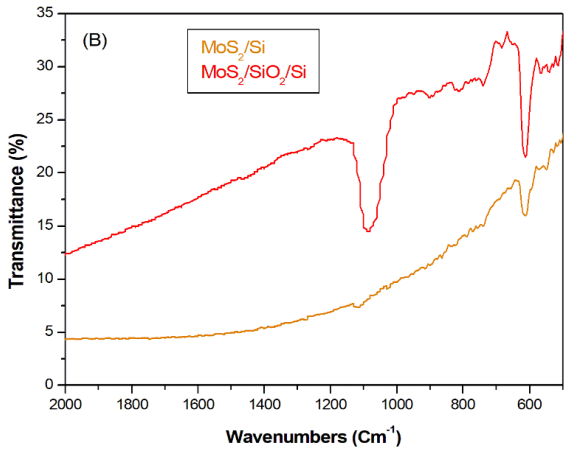

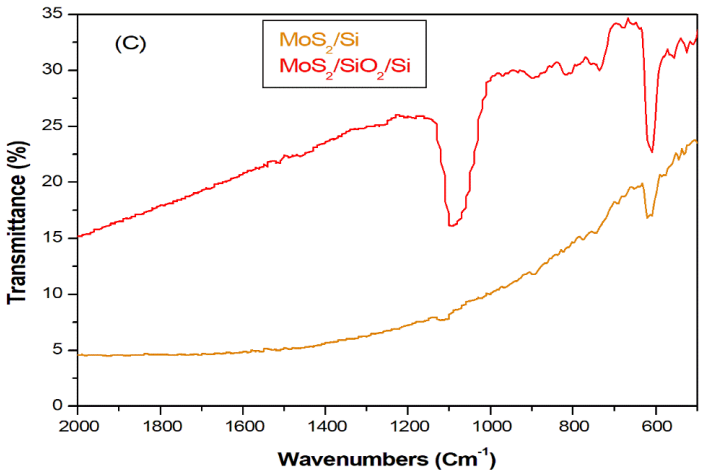

Fig. 3.1 (A) shows the FTIR spectra of MoS_2 on Si and SiO_2/Si substrate at 3000 rpm at 40 sec. (B) MoS_2 on SiO_2/Si and Si substrate at 3000 rpm at 50 sec. (C) MoS_2 on SiO_2/Si and Si substrate at 3000 rpm at 60 sec

The structural characteristics of MoS_2 thin films deposited on Si and SiO_2/Si substrates were analyzed using FTIR spectroscopy. The spectra (Fig. 3a–c) showed a gradual enhancement of Mo–S stretching vibrations as the coating duration increased from 40 s to 60 s at 3000 rpm. For the film coated for 40 s (Fig. 3a), weak and broad Mo–S vibration bands were observed at 567 cm^{-1}, indicating incomplete or thin film formation. At 50 s (Fig. 3b), the characteristic peaks at 567 cm^{-1} and 620 cm^{-1} became more prominent, suggesting improved nucleation and growth. The 60 s film (Fig. 3c) exhibited strong and well-defined Mo–S peaks at 567, 620, 700, and 1150 cm^{-1}, confirming uniform MoS_2 deposition [36].

Additional absorption bands were observed at 1560.19 and 1401.85 cm^{-1} (O–H bending of water and C=O stretching), 950.84 cm^{-1} (CH_2 scissoring), and at 1130.37 and 1039.62 cm^{-1} (asymmetric S–O stretching of sulfate species). A weak peak at 467 cm^{-1} corresponded to Mo–S vibrations on Si. The higher peak intensity on SiO_2/Si at 60 s confirmed better film quality and stronger Mo–S bonding [37].

3.2 Raman Spectroscopy:

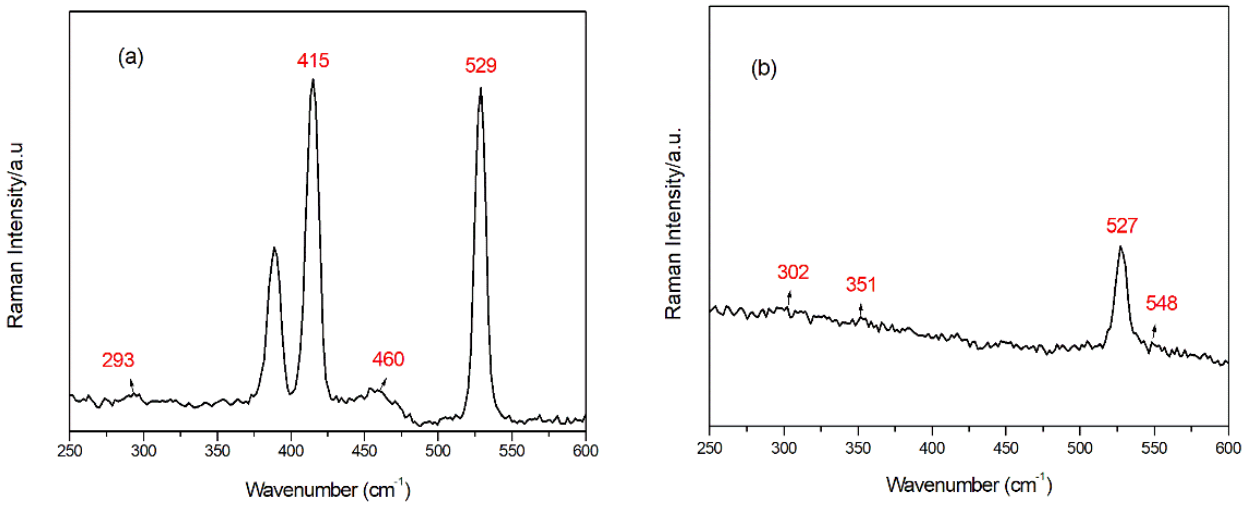

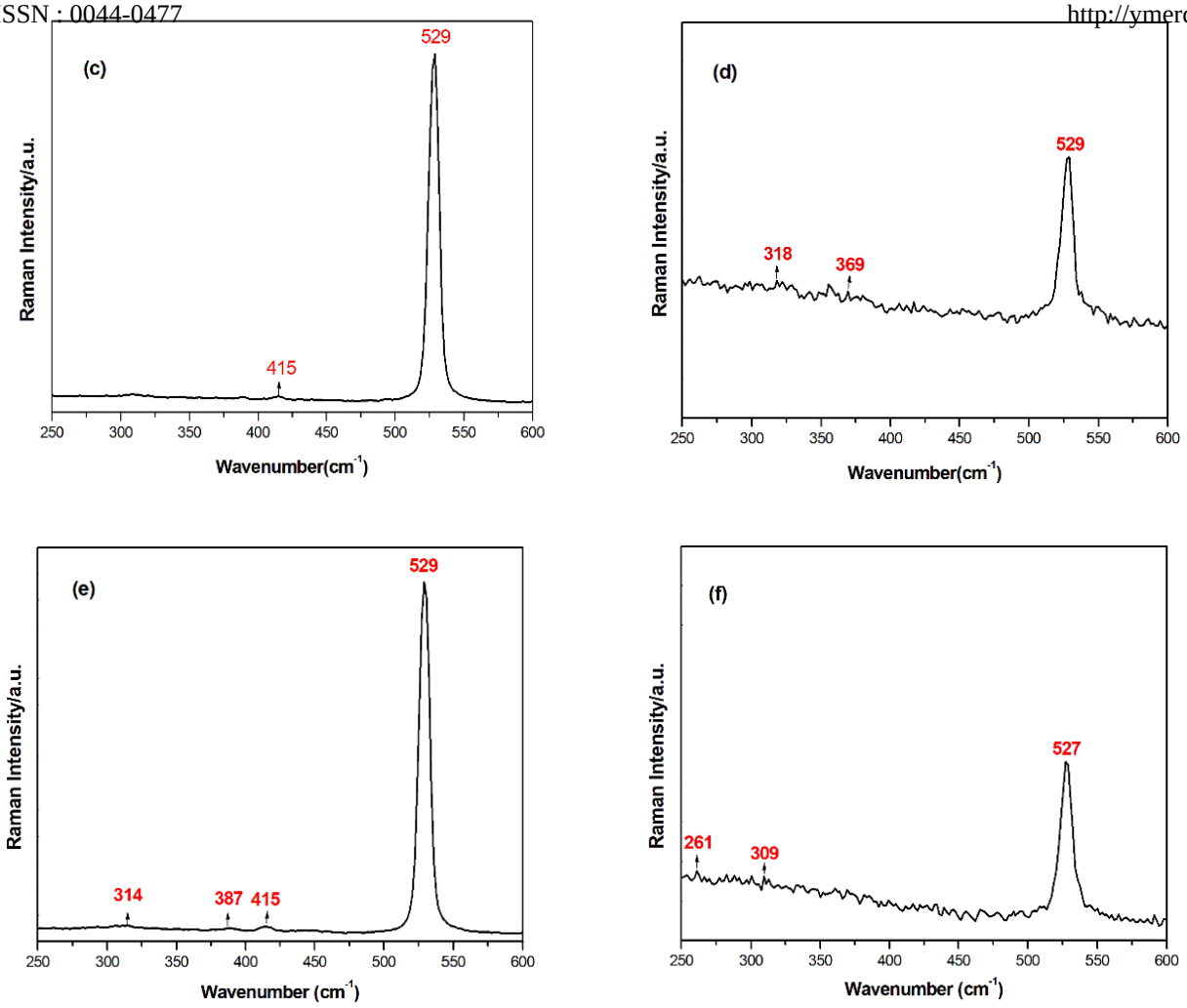

Fig 3.2 shows the Raman spectroscopy of deposited MoS_2 on Si substrate by figure (a, b. c at 40, 50, 60, sec) and MoS_2 on SiO_2/Si at figure (d, e, f at 40, 50 60 sec)

The E_1g E^1_2g, and E^2_2g are in –plane Raman active modes the A_1g is out of plane. The E^1_2g E^1_2g are vibrations of Mo and S planes in opposite direction in the MoS_2 structure, while the E^2_2g are assigned to the vibrations of Mo and S planes in the same direction. The A_1g mode is due to the vibration of only s atoms along the c axis, while the E_1g mode is ascribed to the in plane vibrations of S atoms [38, 22].

In Figure (a), several peaks correspond to the vibrational modes of MoS_2 and the Si substrate. A weak band at about 293 cm^{-1} is due to second-order or defect-activated scattering in MoS_2. This is often seen in few-layer or disordered films [40, 41]. A strong peak at about 387 cm^{-1} matches the in-plane E_2g^1 mode, which comes from the opposite vibrations of Mo and S atoms in the basal plane. The sharp feature at around 415 cm^{-1} is linked to the out-of-plane A_1g mode, related to the vibrations of S atoms along the c-axis [40]. A shoulder-like band near 460 cm^{-1} connects to higher-order phonon combinations [41]. The prominent peak at about 529 cm^{-1} comes from the first-order optical phonon of crystalline Si, showing the substrate's impact. The presence of both E_2g^1 and A_1g modes confirms the 2H-MoS_2 phase, and the frequency difference provides insights

into film thickness, with a larger separation suggesting multilayer growth [42]. **In Figure (b),** additional peaks show up at around 302 and 351 cm^{-1}. The weak band near 302 cm^{-1} is linked to defect-activated phonons of the Mo–S lattice [41], while the 351 cm^{-1} band is associated with second-order or disorder-induced modes that reflect structural flaws. The Si substrate plays a major role with its first-order phonon at about 527 cm^{-1} and a second-order shoulder near 548 cm^{-1} [42]. The lack of clear MoS_2 modes (E_2g^1 and A_1g) points to poor crystallinity or strong masking effects from the substrate. **In Figure (c),** a weak feature at around 415 cm^{-1} corresponds to the A_1g mode of MoS_2, confirming its presence. The sharp and intense band at about 529 cm^{-1} is tied to crystalline Si [42]. The absent E_2g^1 mode at about 385 cm^{-1} indicates that the MoS_2 film is ultrathin, poorly crystalline, or heavily masked by the Si substrate [40, 43]. **In Figure (d),** weak MoS_2 related bands appear at around 318 cm^{-1} (E_2g^1) and 369 cm^{-1} (A_1g), aligning with layered MoS_2 [40, 41]. Their weak intensity suggests limited crystallinity or low thickness. Meanwhile, the strong Si band at about 529 cm^{-1} greatly overshadows the MoS_2 signals [42]. **In Figure (e),** distinct MoS_2 vibrational modes show up at about 387 cm^{-1} (E_2g^1) and 415 cm^{-1} (A_1g), with a frequency difference of about 28 cm^{-1}, typical of multilayer or bulk-like MoS_2 [40]. A weaker mode at around 314 cm^{-1} may result from defect-induced or second-order scattering [41]. Again, the intense Si peak at about 529 cm^{-1} dominates the spectrum [43]. **In Figure (f),** weak MoS_2 related features appear at around 261 and 309 cm^{-1}. They may come from defect-activated or low-frequency phonon processes due to structural disorder or resonance effects [40, 41]. However, the Raman response is mainly influenced by the strong Si phonon at about 527 cm^{-1} [42].

Overall, the Raman spectra confirm the presence of MoS_2 in the deposited thin films. The weaker intensity of its characteristic modes compared to the dominant Si signal suggests partial coverage, low crystallinity, or strong masking effects from the substrate. The occasional detectability of the E_1g mode, even in backscattering geometry, can be attributed to disorder-induced activation, which is often linked to structural defects. Importantly, the presence of the E_2g^1 and A_1g modes unique to crystalline 2H-MoS_2 indicates that the films are not amorphous. Instead, they can be described as partially crystalline (nanocrystalline) MoS_2 with significant disorder/defects, where in some regions the strong Si substrate peak suppresses the MoS_2 response.

3.3 X-Ray Diffraction (XRD):

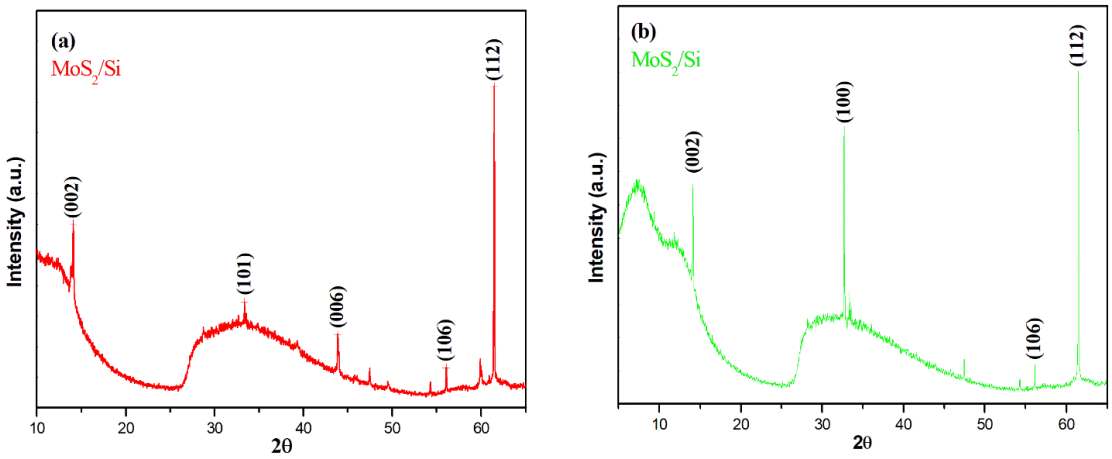

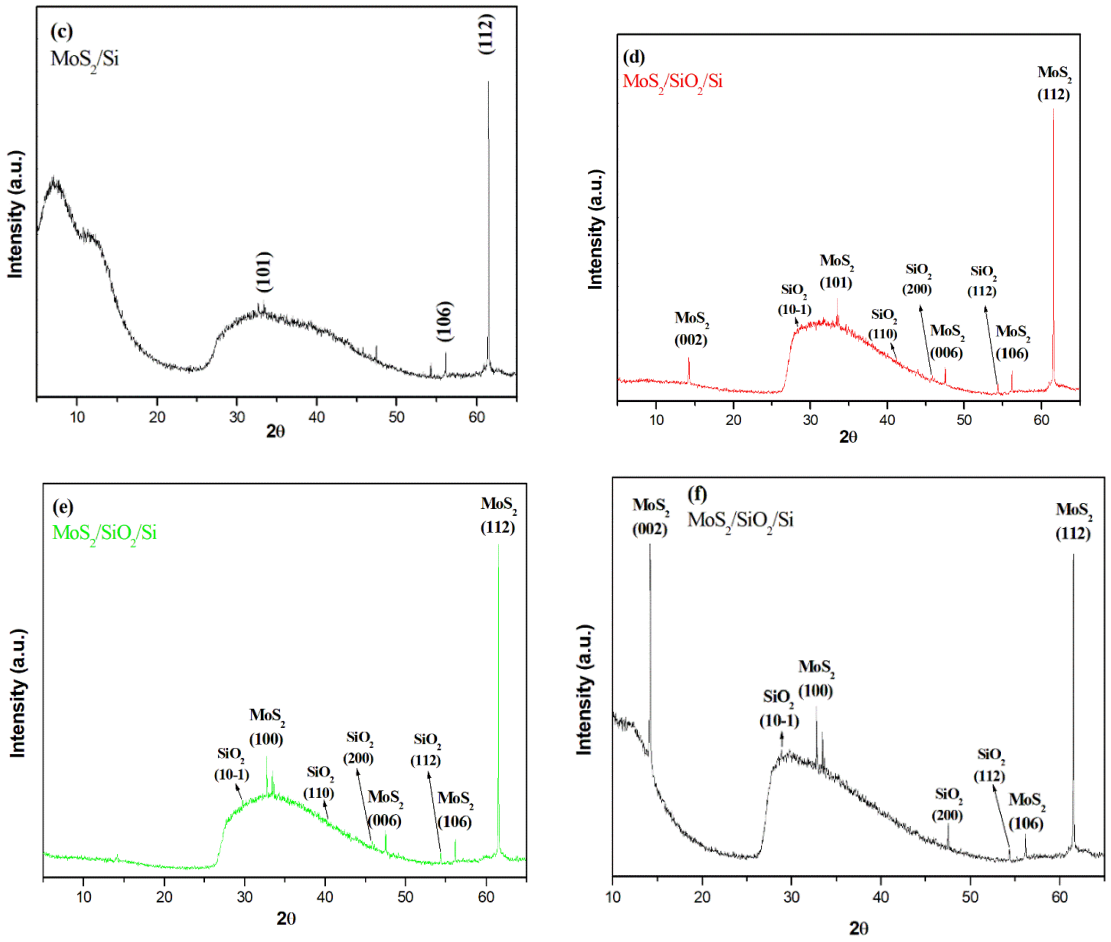

Fig 3.3 X-ray diffraction (XRD) patterns of spin-coated MoS_2 thin films at 3000 rpm showing phase evolution and crystallographic orientation: (a–c) on Si substrate and (d–f) on SiO_2/Si substrate with deposition durations of 40 s, 50 s, and 60 s, respectively.

The X-ray diffraction (XRD) analysis of MoS_2 thin films deposited on Si substrates by spin coating at 3000 rpm for different durations (40 s, 50 s, and 60 s) confirms the formation of the hexagonal 2H-MoS_2 phase along with strong reflections from the crystalline Si substrate. In all samples, characteristic MoS_2 peaks are observed at 14.4° ((002) basal plane), 33–34° ((100) in-plane), 39–40° ((103)), and a weaker reflection near 58°, which correspond well with the standard JCPDS card No. 96-101-0994. The dominant peaks of the Si substrate appear at 28.4° (Si (111)), 47.3° (Si (220)), and 56.1° (Si (311)), matching JCPDS card No. 27-1402. At 40 s deposition, the MoS_2 reflections are relatively weak and broadened, indicating incomplete surface coverage, nanoscale crystallite size, and possible micro strain effects. When the deposition time is increased to 50 s, the MoS_2 peaks become more prominent, confirming the formation of crystalline hexagonal 2H-MoS_2, although the strong Si reflections still dominate the pattern, suggesting a thin film. For the longest deposition time of 60 s (sample S3), the MoS_2 peaks exhibit slightly enhanced intensity, pointing toward improved crystallinity and better surface

coverage, although the film thickness remains limited compared to the strong Si background. Such peak broadening and crystallinity evolution trends have also been reported in earlier studies on spin-coated MoS_2 thin films [44, 45]. Overall, the XRD results confirm the successful deposition of hexagonal 2H-MoS_2 on Si substrates, with crystallinity and coverage gradually improving as the spin-coating duration increases from 40 to 60s.

MoS_2 thin films were successfully deposited on SiO_2/Si substrates using a spin-coating technique at a constant speed of 3000 rpm, with deposition times of 40, 50, and 60 s. The X-ray diffraction (XRD) patterns of all samples revealed distinct reflections characteristic of hexagonal 2H-MoS_2, consistent with the standard JCPDS card No. 37-1492. Prominent peaks observed at 14.2°, 32.8°, 39.6°, and 58.9° were indexed to the (002), (100), (103), and (112) planes of MoS_2 confirming the layered crystalline nature of the deposited films. A broad hump appearing in the 20–25° region was attributed to the amorphous SiO_2 layer of the substrate, which is a common feature in thermally grown or deposited SiO_2/Si systems, and this background contribution enabled clear distinction of the MoS_2 reflections. With increasing spin time, the XRD patterns demonstrated enhanced crystallinity and preferential orientation along the c-axis, as indicated by the more intense (002) reflection, while the absence of additional impurity peaks confirmed the phase purity of the films. These findings are in good agreement with earlier studies on spin-coated MoS_2 thin films [46-48].

4. Conclusion:

MoS_2 thin films were successfully deposited on Si and SiO_2/Si substrates using the spin-coating method, and their structural and vibrational properties were systematically characterized. FTIR analysis confirmed the progressive development of Mo–S vibrational modes with increasing coating duration, indicating improved nucleation and uniformity. Raman spectroscopy revealed the characteristic E_2g^1 and A_1g modes of 2H-MoS_2, with their weak intensity pointing to partial coverage, nanocrystallinity, and substrate influence. XRD patterns validated the presence of crystalline hexagonal 2H-MoS_2, with enhanced crystallinity and preferential c-axis orientation observed at longer deposition times, while AFM supported these findings by highlighting surface morphology and film uniformity. Overall, the results demonstrated that SiO_2/Si substrates favored better layer formation, uniform deposition, and stronger Mo–S bonding compared to bare Si, emphasizing the critical role of substrate choice in tailoring film quality. These findings provide useful insights for optimizing spin-coated MoS_2 thin films for future electronic and optoelectronic device applications.

5. Acknowledgments:

One of the authors, Vaibhav Borokar, would like to thanks the Chhatrapati Shahu Maharaj National Research, Training and Human Development Institute (SARTHI) Pune for providing financial support. Authors are gratefully to RUSA center at BAMU University for the Characterization support.

6. Reference:

1. J. Sun, X. Li, W. Guo, M. Zhao, X. Fan, Y. Dong and Y. Fu, "Synthesis methods of two-dimensional MoS_2: A brief review", Crystals. vol. 7, no. 7, (2017), pp. 198.

2. R. T. Busch, L. Sun, D. Austin, J. Jiang, P. Miesle, M. A. Susner and P. R. Stevenson, "Exfoliation procedure-dependent optical properties of solution deposited MoS_2 films", npj 2D Materials and Applications. vol. 7, no. 1, (2023), pp. 12.

3. X. Xiaoli, "A review: the method for synthesis MoS2 monolayer", International Journal of Nano manufacturing. vol. 10, no. 5–6, (2014), pp. 489–499**.**

4. P. Joensen, R. F. Frindt and S. R. Morrison, "Single-layer MoS_2", Materials Research Bulletin. vol. 21, no. 4, (1986), pp. 457–461.

5. A. K. Dabral, A. Lu, D. Chiappe, M. Houssa and G. Pourtois, "Scaling challenges in advanced Si devices", Physical Chemistry Chemical Physics. (2019), DOI: 10.1039/c8cp05665j.

6. Z. Lin et al., "2D Materials growth and properties", 2D Materials. vol. 3, no. 4, (2016), 042001.

7. P. Zhou, S. Yang, Q. Sun, L. Chen, P. Wang, S. Ding and D. W. Zhang, "2D/oxide interface properties", Scientific Reports. (2014), DOI: 10.1038/srep06448.

8. H. G. Kim and H. B. R. Lee, "MoS_2 structural characteristics", Chemistry of Materials. (2017), DOI: 10.1021/acs.chemmater.6b05103.

9. S. M. George, "Atomic layer deposition: an overview", Chemical Reviews. vol. 110, no. 1, (2010), pp. 111–131.

10 G. N. Parsons et al., "History of atomic layer deposition", Journal of Vacuum Science & Technology A. vol. 31, no. 5, (2013).

11. J. E. Crowell, "Chemical methods of thin film deposition", Journal of Vacuum Science & Technology A. vol. 21, no. 5, (2003), pp. S88–S95.

12. K. S. Agrawal, V. S. Patil, A. G. Khairnar and A. M. Mahajan, "CeO_2 thin films for MOS capacitors", Journal of Materials Science: Materials in Electronics. vol. 28, (2017), pp. 12503–12508.

13. V. N. Barhate, K. S. Agrawal, V. S. Patil and A. M. Mahajan, "Annealed La-doped cerium oxide thin films", Rare Metals. vol. 40, no. 7, (2021), pp. 1835–1843.

14. V. Barhate, K. Agrawal, V. Patil, S. Patil and A. Mahajan, "Spectroscopic study of La_2O_3 films", International Journal of Modern Physics B. vol. 32, no. 19, (2018), 1840074.

15. V. Y. Borokar, V. Barhate, B. Desale and A. Mahajan, "Growth of PEALD La_2O_3 on SiO_2/Si", International Journal of Modern Physics B. vol. 38, no. 12–13, (2024), 2440017.

16. H. Li, J. Wu, Z. Yin and H. Zhang, "Mechanically exfoliated MoS_2 nanosheets", Accounts of Chemical Research. vol. 47, no. 4, (2014), pp. 1067–1075.

17. C. Muratore et al., "Ultra-thin MoS_2 films by PVD", Applied Physics Letters. vol. 104, no. 26, (2014).

18. Z. Zhu et al., "MoS_2 growth by CVD", Materials Research Express. vol. 6, no. 9, (2019), 095011.

19. R. Kaindl et al., "Sputter-deposited MoS_2 films", Beilstein Journal of Nanotechnology. vol. 8, (2017), pp. 1115–1126.

20. J. Huang et al., "Large-area MoS_2 by sputtering", Materials Research Express. vol. 3, no. 6, (2016), 065007.

21. J. Pütz and M. A. Aegerter, "Spin deposition of MoSx films", Thin Solid Films. vol. 351, no. 1–2, (1999), pp. 119–124.

22. G. G. Politano et al., "Spin-coated MoS_2 films investigation", Materials Proceedings. vol. 3, no. 1, (2020).

23. G. G. Politano et al., "Ellipsometry of spin-coated MoS_2", Vacuum. vol. 189, (2021), 110232.

24. Engineering & Science. vol. 38, no. 12, (1998), pp. 2039–2045.

25. C. J. Lawrence, "Mechanics of spin coating", Physics of Fluids. vol. 31, no. 10, (1988), pp. 2786–2795.

26. D. B. Mitzi et al., "High-mobility films by spin coating", Nature. vol. 428, (2004), pp. 299–303.

27. P. He et al., "Devices from solution-processed 2D materials", in Synthesis & Modeling of 2D Materials, Elsevier, (2020), pp. 351–384.

28. H. Li et al., "Raman evolution from bulk to monolayer MoS_2", Advanced Functional Materials. vol. 22, (2012), pp. 1385–1390.

29. S. Reshmi et al., "Structural stability of 1T-2H MoS_2", Nanotechnology. vol. 29, (2018), 205604.

30. G. Eda et al., "2H/1T MoS_2 heterostructures", ACS Nano. vol. 6, (2012), pp. 7311–7317.

31. V. Nicolosi et al., "Liquid exfoliation of layered materials", Science. vol. 340, (2013), 1226419.

32. N. D. Mansukhani et al., "High-concentration 2D dispersions", Small. vol. 12, (2016), pp. 294–300.

33. G. Y. Jia et al., "Quantum confined optical conductivity of MoS_2", Journal of Materials Chemistry C. vol. 4, no. 37, (2016), pp. 8822–8828.

34. O. Lopez-Sanchez et al., "MoS_2 photodetectors", Nature Nanotechnology. vol. 8, no. 7, (2013), pp. 497–501.

35. T. Han et al., "Optical properties of MoS_2 on substrates", Nanomaterials. vol. 9, no. 5, (2019), pp. 740.

36. G. A. Ali et al., "MoS_2/graphene for supercapacitors", Journal of Solid State Electrochemistry. vol. 24, (2020), pp. 25–34.
37. X. Feng et al., "Solvothermal synthesis of MoS_2 nanosheets", Crystal Research and Technology. vol. 48, no. 6, (2013), pp. 363–368.
38. Z. H. Chi et al., "Pressure-induced MoS_2 metallization", Physical Review Letters. vol. 113, (2014), 036802.
39. C. Lee et al., "Lattice vibrations in MoS_2", ACS Nano. vol. 4, no. 5, (2010), pp. 2695–2700.
40. H. Terrones et al., "Hetero-layered metal disulfides", Scientific Reports. vol. 3, (2013), 1549.
41. I. De Wolf, "Raman study of stress in Si circuits", Semiconductor Science and Technology. vol. 11, no. 2, (1996), pp. 139–154.
42. H. Li et al., "Optical identification of MoS_2 layers", Small. vol. 8, no. 5, (2012), pp. 682–686.
43. A. Roy et al., "Pulsed laser deposited MoS_2 properties", ACS Applied Materials & Interfaces. vol. 6, no. 4, (2014), pp. 2534–2540.
44. S. Ghatak, A. N. Pal and A. Ghosh, "Electronic states in MoS_2 FETs", ACS Nano. vol. 5, no. 10, (2011), pp. 7707–7712.
45. A. Gupta, T. Sakthivel and S. Seal, "2D materials beyond graphene", Progress in Materials Science. vol. 73, (2015), pp. 44–126.
46. D. J. Late et al., "Hysteresis in MoS_2 FETs", ACS Nano. vol. 6, no. 6, (2012), pp. 5635–5641.
47. Y. Yu et al., "Scalable synthesis of MoS_2 films", Scientific Reports. vol. 3, (2013), 1866.